Inorg. Chem. **2008**, *47*, 2121−2132

Zinc(II), Cadmium(II), Mercury(II), and Ethylmercury(II) Complexes of Phosphinothiol Ligands

P. Fernández,[†] A. Sousa-Pedrares,[†] J. Romero,[†] J. A. García-Vázquez,[*,†] A. Sousa,[†] and P. Pérez-Lourido[‡]

Departamento de Química Inorgánica, Universidad de Santiago de Compostela, 15782, Santiago de Compostela, Spain, and Departamento de Química Inorgánica, Universidad de Vigo, 36200 Vigo, Spain

Received March 29, 2007

Neutral zinc, cadmium, mercury(II), and ethylmercury(II) complexes of a series of phosphinothiol ligands, $Ph_nP(C_6H_3(SH\text{-}2)(R\text{-}3))_{3-n}$ (n = 1, 2; R = H, $SiMe_3$) have been synthesized and characterized by IR and NMR (^1H, ^{13}C, and ^{31}P) spectroscopy, FAB mass spectrometry, and X-ray structural analysis. The compounds $[Zn\{PhP(C_6H_4S\text{-}2)_2\}]$ (**1**) and $[Cd\{Ph_2PC_6H_4S\text{-}2\}_2]$ (**2**) have been synthesized by electrochemical oxidation of anodic metal (zinc or cadmium) in an acetonitrile solution of the appropriate ligand. The presence of pyridine in the electrolytic cell affords the mixed complexes $[Zn\{PhP(C_6H_4S\text{-}2)_2\}(py)]$ (**3**) and $[Cd\{PhP(C_6H_4S\text{-}2)_2\}(py)]$ (**4**). $[Hg\{Ph_2PC_6H_4S\text{-}2\}_2]$ (**5**) and $[Hg\{Ph_2PC_6H_3(S\text{-}2)(SiMe_3\text{-}3)\}_2]$ (**6**) were obtained by the addition of the appropriate ligand to a solution of mercury(II) acetate in methanol in the presence of triethylamine. $[EtHg\{Ph_2PC_6H_4S\text{-}2\}]$ (**7**), $[EtHg\{Ph_2P(O)C_6H_3(S\text{-}2)(SiMe_3\text{-}3)\}]$ (**8**), $[\{EtHg\}_2\{PhP(C_6H_4S\text{-}2)_2\}]$ (**9**), and $[\{EtHg\}_2\{PhP(C_6H_3(S\text{-}2)(SiMe_3\text{-}3))_2\}]$ (**10**) were obtained by reaction of ethylmercury(II) chloride with the corresponding ligand in methanol. In addition, in the reactions of EtHgCl with $Ph_2PC_6H_4SH\text{-}2$ and with the potentially tridentate ligand $PhP(C_6H_3(SH\text{-}2)(SiMe_3\text{-}3))_2$, cleavage of the Hg−C bond was observed with the formation of $[Hg\{Ph_2PC_6H_4S\text{-}2\}_2]$ (**5**) and $[Hg(EtHg)_2\{PhP(O)(C_6H_3(S\text{-}2)(SiMe_3\text{-}3))_2\}_2]$ (**11**), respectively, and the corresponding hydrocarbon. The crystal structures of $[Zn_3\{PhP(C_6H_4S\text{-}2)_2\}_2\{PhP(O)(C_6H_4S\text{-}2)_2\}]$ (**1***), $[Cd_2\{Ph_2PC_6H_4S\text{-}2\}_3\{Ph_2P(O)C_6H_4S\text{-}2\}]$ (**2***), **3**, **5**, **6**, $[EtHg\{Ph_2P(O)C_6H_4S\text{-}2\}]$ (**7***), **8**, **9**, $[\{EtHg\}_2\{PhP(O)(C_6H_3(S\text{-}2)(SiMe_3\text{-}3))_2\}]$ (**10***), and **11** are discussed. The molecular structures of **1**, **2**, **4**, **7**, and **10** have also been studied by means of density functional theory (DFT) calculations.

Introduction

The chemistry of metal−sulfur complexes has attracted a great deal of interest over the past decade because of the potential relevance of such compounds to active sites in metalloenzymes and their ability to adopt geometries of variable nuclearity and great structural complexity.[1–7] The chemistry of mercury complexes containing ligands bearing sulfur atoms is related to mercury−cysteine thionato interactions in the toxicological behavior of this metal,[8] in detoxification of the mercury by metallothioneins[9] in a DNA-binding protein,[10] and in mercury reductase and related proteins.[6,11]

Zinc and cadmium metals with thiolate ligands usually form polymeric species as a consequence of the tendency of thiolato ligands to bridge metal centers. Thus, neutral thiolate $[M(SR)_2]$ complexes of zinc or cadmium generally

* To whom correspondence should be addressed. Tel: +34-981563100, ext 14950. Fax: + 34-(9)81 594912. E-mail: qijagv@usc.es.
† Universidad de Santiago de Compostela.
‡ Universidad de Vigo.

(1) Raper, E. S. *Coord. Chem. Rev.* **1985**, *61*, 115–184.
(2) Raper, E. S. *Coord. Chem. Rev.* **1996**, *153*, 199–225.
(3) Raper, E. S. *Coord. Chem. Rev.* **1997**, *165*, 475–567.
(4) Krebs, B.; Henkel, G. *Angew. Chem., Int. Ed. Engl.* **1991**, *30*, 769–788.
(5) Dance, I. G. *Polyhedron* **1986**, *5*, 1037–1104.
(6) Blower, P. G.; Dilworth, J. R. *Coord. Chem. Rev.* **1987**, *76*, 121–185.
(7) Dilworth, J. R.; Hu, J. *Adv. Inorg. Chem.* **1993**, *40*, 411–459.
(8) Cheesman, B. V.; Arnold, A. P.; Rabenstein, D. L. *J. Am. Chem. Soc.* **1988**, *110*, 6359–6364.
(9) (a) Nielson, K. B.; Atkin, C. L.; Winge, D. R. *J. Biol. Chem.* **1985**, *260*, 5342–5350. (b) Stillman, M. J.; Law, A. Y. C.; Szymanska, J. A. *Chemical Toxicology and Clinical Chemistry of Metals*; Academic Press, London, 1983, p 275. (c) Vasak, M.; Kagi, J. H. R.; Hill, H. A. O. *Biochemistry* **1981**, *20*, 2852–2856.
(10) Dance, I. G. *Polyhedron* **1986**, *5*, 1037–1104.
(11) Gopinath, E.; Kaaret, T. W.; Bruice, T. C. *Proc. Natl. Acad. Sci. U.S.A.* **1989**, *86*, 3041–3044.

10.1021/ic7005925 CCC: $40.75
Published on Web 02/14/2008

form infinite lattices with bridging ligands and tetrahedral metal centers.[12] The polymeric nature of these systems leads to insoluble compounds that are difficult to isolate as crystals suitable for X-ray studies, and they are also unsuitable as precursors for metal calcogenides under typical metal−organic chemical vapor deposition (MOCVD) conditions. The aggregation phenomena can be controlled by steric constraints produced by appropriate ligand design[13] or by saturation of the metal coordination sphere with other donor atoms in addition to the thiolate group. In the specific cases of multidentate mixed-donor ligands, complex stability is enhanced by chelating effects. In previous studies, we have used this strategy for the synthesis of monomeric[14] and dimeric compounds[15] of zinc and cadmium with sterically hindered heterocyclic thiones.

Inorganic mercury(II) complexes exhibit a wide range of coordination numbers and environments, while organomercury $[RHg]^+$ compounds (e.g., ethylmercury(II) complexes) almost invariably contain the metal in a linear two coordinate geometry[16] with, in some cases, additional weak secondary bonds.[17] It is well-known that the metal–carbon bond in $[RHg]^+$ compounds is rather stable,[18] and this stability under physiological conditions, along with its lipophilic nature, leads to a strong tendency toward bioaccumulation in the food chain. However, the bacterial enzyme organomercurial lyase (MerB) catalyzes the protonolytic cleavage of $[RHg]^+$ cations to yield the parent hydrocarbon and inorganic Hg(II), which is complexed through thiolate groups.[19] It seems that the initial formation of an enzyme–substrate complex in the organomercurial lyase active site polarizes the Hg−C bond, favoring attack by the electrophilic agent and cleavage of the bond itself. Some recent studies have confirmed that the activation of the Hg−C bond and its cleavage is related to the coordination of mercury by strongly donating ligands such as $N(CH_2CH_2PPh_2)_3$,[20] 2-(2′-pyridyl)quinoxaline,[21] diphenyldithiophosphinic acid,[22] and thioethers.[23]

Polydentate ligands incorporating both thiolate and tertiary phosphine donor atoms form stable complexes with a wide range of metals including lanthanides and transition and post-transition metals. To date, most studies have focused on bidentate $Ph_2PCH_2CH_2SH$ or $Ph_2PC_6H_4SH$-2 ligands,[24] while the potentially tridentate ligand $PhP(C_6H_4SH\text{-}2)_2$ has received less attention. Some studies on the chemistry of zinc and cadmium with these ligands have already been published,[25] but mercury(II) or ethylmercury(II) complexes with phosphinothiol ligands have not been reported.

In this paper, we describe the electrochemical synthesis and characterization of new zinc and cadmium compounds with arenephosphinothiol ligands in which the polydentate behavior of the ligand and the presence of additional coligands allows the preparation of low molecular species. In addition, the chemistry of Hg(II) and $[EtHg]^+$ with these ligands is also explored. In the reaction of EtHgCl with some of these ligands, the initial products are unstable in solution and undergo oxidation and cleavage processes leading to the formation of inorganic mercury(II) thiolates.

Experimental Section

General Considerations. All manipulations were carried out under an inert atmosphere of dry nitrogen. Zinc and cadmium (Aldrich Chemie) were used as plates (ca. 2 × 2 cm). Mercury acetate and ethylmercury chloride (Aldrich Chemie) were used as provided. All other reagents were used as supplied. Synthesis of ligands was carried out using slight modifications of the standard literature procedure.[26] Elemental analyses were performed using a Perkin-Elmer 240B microanalyzer. IR spectra were recorded as KBr discs using a Perkin-Elmer spectrophotometer. ^1H, ^{13}C, and ^{31}P spectra were recorded on a Bruker WM 350 MHz instrument using $CDCl_3$ as solvent. ^1H NMR and ^{13}C chemical shifts were determined against trimethylsilane (TMS) as internal standard and those of ^{31}P against 85% H_3PO_4. The mass spectra (FAB) were recorded on a Micromass Autospec spectrometer using 3-nitrobenzyl alcohol as the matrix material.

Electrochemical Synthesis of Zinc and Cadmium Compounds. The zinc and cadmium complexes **1**–**4** were obtained using an electrochemical procedure.[27] The cell consisted of an anode suspended from a platinum wire, and the cathode was also a platinum wire. The ligand was dissolved in acetonitrile and a small amount of tetramethylammonium perchlorate was added to the solution as a supporting electrolyte (**Caution**: *perchlorate compounds are potentially explosive and should be handled in small quantities and with great care*). For the synthesis of mixed complexes, pyridine was also added to the solution. Applied voltages of 10–15 V allowed sufficient current flow for smooth dissolution of the metal. During electrolysis, nitrogen was bubbled

(12) (a) Craig, D. C.; Dance, I. G.; Garbutt, R. G. *Angew. Chem., Int. Ed. Engl.* **1986**, *98*, 178–179. (b) Dance, I. G.; Garbutt, R. G.; Graig, D. C.; Scudder, M. L. *Inorg. Chem.* **1987**, *26*, 4057–4064.

(13) Bochman, M.; Bwembya, G.; Grinter, R. R.; Lu, J.; Webb, K.; Willianson, D. J.; Hursthouse, M. H.; Mazid, M. *Inorg. Chem.* **1993**, *32*, 532–537.

(14) Castro, R.; Durán, M. L.; García-Vázquez, J. A.; Romero, J.; Sousa, A.; Castiñeiras, A.; Hiller, W.; Strahle, J. *Z. Naturforsch.* **1992**, *47b*, 1067–1074.

(15) Castro, R.; García-Vázquez, J. A.; Romero, J.; Sousa, A.; Castiñeiras, A.; Hiller, W.; Strahle, J. *Inorg. Chim. Acta* **1993**, *211*, 47–54.

(16) Wardell, J. L. In *Comprehensive Organometallic Chemistry*; Wilkinson, G., Ed.; Pergamon Press: Oxford, U.K., 1982; Vol. *2* p 901.

(17) (a) Casas, J. S.; García-Tasende, M. S.; Sordo, J. *Coord. Chem. Rev.* **1999**, *193–195*, 283–359. (b) Holloway, C. E.; Melnik, M. *J. Organomet. Chem.* **1995**, *495*, 1–31. (c) Tallon, J.; García-Vázquez, J. A.; Romero, J.; Louro, M. S.; Sousa, A. *Polyhedron* **1995**, *114*, 2309–2317. (d) Atwood, J. O.; Berry, D. E.; Stobard, S. R;.; Zoworotko, M. J. *Inorg. Chem.* **1983**, *22*, 3480–3482. (e) Black, D. St.; Deacon, G. B.; Edwards, G. L.; Gatehouse, M. *Aust. J. Chem.* **1993**, *46*, 1323–1326.

(18) Bloodworth, A. J. In *The Chemistry of Mercury*; McAuliffe, C. A., Ed.; Mc Millan Press: London, 1977; Chapter 22, pp 209–233.

(19) Moore, M. J.; Distefano, M. D.; Zydowsky, L. D.; Cummings, R. T.; Walsh, C. T. *Acc. Chem. Res.* **1990**, *23*, 301–308.

(20) Barbaro, P.; Cecconi, F.; Ghilardi, C. A.; Midollini, S.; Orlandini, A.; Vacca, A. *Inorg. Chem.* **1994**, *33*, 6163–6170.

(21) Garoufis, A.; Perlepes, S. S.; Scheiber, A.; Bau, R.; Hadjiliadis, N. *Polyhedron* **1996**, *15*, 177–180.

(22) Casas, J. S.; García-Tasende, M. S.; Sánchez, A.; Sordo, J.; Vázquez-López, E. M. *Inorg. Chim. Acta* **1997**, *256*, 211–216.

(23) Wilhelm, M.; Deeken, S.; Berssen, E.; Saak, W.; Lützen, A.; Koch, R.; Strasdeit, H. *Eur. J. Inorg. Chem.* **2004**, 2301–2312.

(24) Dilworth, J. R.; Wheatley, N. *Coord. Chem. Rev.* **2000**, *199*, 89–158, and references therein.

(25) Pérez-Lourido, P.; Romero, J.; García-Vázquez, J. A.; Sousa, A.; Maresca, K.; Zubieta, J. *Inorg. Chem.* **1999**, *38*, 3709–3715.

(26) Block, E.; Ofori-Okai, G.; Zubieta, J. *J. Am. Chem. Soc.* **1989**, *111*, 2327–2329.

(27) (a) Tuck, D. G. *Pure Appl. Chem.* **1979**, *51*, 2005–2018. (b) Chakravorti, M. C.; Subrahmanyam, G. V. B. *Coord. Chem Rev.* **1994**, *135–136*, 65–92. (c) Vecchio-Sadus, A. M. *J. Appl. Electrochem.* **1993**, *23*, 401–416.

through the solution to provide an inert atmosphere and also to stir the reaction mixture. In these conditions, the electrochemical cell can be summarized as

$$Pt_{(-)}/CH_3CN + Ph_nP(C_6H_3(SH\text{-}2)(R\text{-}3))_{3-n}/M_{(+)};\ M = Zn,Cd \quad (1)$$

Synthesis of [Zn{PhP(C_6H_4S-2)$_2$}] (1). Electrochemical oxidation of a zinc anode in a solution of PhP(C_6H_4SH-2)$_2$ (0.122 g, 0.374 mmol) in acetonitrile (50 mL) at 12 V, 10 mA, for 2 h caused 24.0 mg of zinc to be dissolved; E_f = 0.49 mol F^{-1}. During the electrolysis, hydrogen was evolved at the cathode, and at the end of the reaction, a white crystalline solid appeared at the bottom of the vessel. The solid was filtered off, washed with acetonitrile and ether, and dried under vacuum. Anal. Calcd for $C_{18}H_{13}PS_2Zn$ (mol wt 387.9): C, 55.67; H, 3.38; S, 16.48. Found: C, 54.97; H, 3.50; S, 15.98%. IR (cm^{-1}): 1574(m), 1440(s), 1421(s), 1253(m), 1101(s), 744(s), 694(m). ^{1}H NMR ($CDCl_3$, ppm): δ 7.9–6.6 (m, 13H). ^{31}P NMR ($CDCl_3$, ppm): δ 29.3. FAB MS: *m*/*z* 389 (ZnL^+); 778 ($Zn_2L_2^+$); 1167 ($Zn_3L_3^+$). Crystals of [Zn_3{PhP(C_6H_4S-2)$_2$}$_2${PhP(O)(C_6H_4S-2)$_2$}] (**1***) suitable for X-ray analysis were obtained by concentration of the mother liquor.

Synthesis of [Cd{$Ph_2PC_6H_4$S-2}$_2$] (2). A similar experiment (13 V, 10 mA, 2 h) with cadmium as the anode and $Ph_2PC_6H_4$SH-2 (0.220 g, 0.748 mmol) in acetonitrile (50 mL) dissolved 40 mg of metal (E_f = 0.47 mol F^{-1}). At the end of the electrolysis, the white crystals deposited in the cell were recovered, washed with cool acetonitrile and diethyl ether, and dried under vacuum. Anal. Calcd for $C_{36}H_{28}P_2S_2Cd$ (mol wt 700.0): C, 61.71; H, 4.03; S, 9.13. Found: C, 62.80; H, 4.20; S, 9.33%. IR (KBr, cm^{-1}): 1570(m), 1479(m), 1435(s), 1418(m), 1247(m), 1094(m), 743(s), 693(s). ^{1}H NMR (CD_3Cl, ppm): δ 8.0–6.8 (m, 28H). ^{31}P NMR ($CDCl_3$, ppm): δ 35.2. Crystals of [Cd_2{$Ph_2PC_6H_4$S-2}$_3${Ph_2P(O)C_6H_4S-2}]·CH_3CN (**2***) suitable for X-ray studies were obtained by concentration of the mother liquor.

Synthesis of [Zn{PhP(C_6H_4S-2)$_2$}(py)] (3). Electrolysis of an acetonitrile solution (50 mL) containing PhP(C_6H_4SH-2)$_2$ (0.124 g, 0.378 mmol) and pyridine (0.031 g, 0.380 mmol) using a current of 10 mA (12 V) for 2 h led to the dissolution of 25 mg of zinc (E_f = 0.50 mol F^{-1}). The crystalline solid obtained was washed with acetonitrile and ether and dried under vacuum. Anal. Calcd for $C_{23}H_{18}NPS_2Zn\cdot CH_3CN$ (mol wt 508.0): C, 59.05; H, 4.17; S, 12.59; N, 5.51. Found: C, 58.55; H, 4.06; S, 12.66, N, 5.31%. IR (cm^{-1}): 1605(m), 1573(m), 1447(s), 1438(s), 1417(s), 1247(m), 1220(m), 1156(s), 1134(s), 998(m), 743(s), 665(m). ^{1}H NMR ($CDCl_3$, ppm): δ 8.0–6.8(m, 18 H). ^{31}P NMR ($CDCl_3$, ppm): δ 39.9. FAB MS: *m*/*z* 389 (ZnL^+); 778 ($Zn_2L_2^+$); 1167 ($Zn_3L_3^+$). Crystals of [Zn_2{PhP(C_6H_4S-2)$_2$}$_2$(py)$_2$]·$2CH_3CN$ suitable for X-ray studies were obtained directly from the cell.

Synthesis of [Cd{PhP(C_6H_4S-2)$_2$}(py)] (4). The same procedure was used for the synthesis of this compound. A solution of the ligand (0.122 g, 0.374 mmol) and pyridine (0.030 g, 0.379 mmol) in acetonitrile (50 mL) was electrolyzed at 10 mA during 1 h, and 21 mg of the metal was dissolved from the anode (E_f = 0.50 mol F^{-1}). Anal. Calcd for $C_{23}H_{18}NPS_2Cd$ (mol wt 516.9): C, 53.54; H, 3.51; S, 12.41; N, 2.71. Found: C, 53.84; H, 3.80; S, 12.50, N, 2.90%. IR (KBr, cm^{-1}): 1630(m), 1581(m), 1437(m), 1418(m), 1227(m), 1121(s), 1107(s), 997(m), 745(s), 694(m).^{1}H NMR ($CDCl_3$, ppm): δ 8.0–6.8 (m, 18 H). ^{31}P NMR ($CDCl_3$, ppm): δ 39.9. FAB MS: *m*/*z* 436 (CdL^+), 872 ($Cd_2L_2^+$).

Synthesis of Mercury Compounds. Mercury(II) and ethylmercury(II) complexes were obtained by slow addition to a stirred solution of the appropriate ligand and triethylamine in methanol of a solution of mercury acetate (for the synthesis of complexes **5** and **6**) or a solution of ethylmercury(II) chloride in the same solvent (for complexes **7**–**10**).

Synthesis of [Hg{$Ph_2PC_6H_4$S-2}$_2$] (5). To a stirred solution of $Ph_2PC_6H_4$SH-2 (0.10 g, 0.34 mmol) and NEt_3 (0.048 mL, 0.35 mmol) in methanol (25 mL) was added slowly a solution of mercuric acetate (0.054 g, 0.17 mmol) in methanol (15 mL) at room temperature. In a few minutes, a white solid was formed. The solid was filtered off, washed with methanol, and dried *in vacuo*. Anal. Calcd for $C_{36}H_{28}P_2S_2Hg$ (mol wt 788.1): C, 54.82; H, 3.58; S, 8.11. Found: C, 55.12; H, 3.61; S, 7.88%. IR (KBr, cm^{-1}): 1573(m), 1478(m), 1437(s), 1415(m), 1093(s), 743(s), 695(s), 523(s), 502(m), 470(m). ^{1}H NMR ($CDCl_3$, ppm): δ 7.7–6.9 (m, 28H). ^{13}C NMR ($CDCl_3$, ppm): δ 134–124. ^{31}P NMR ($CDCl_3$, ppm): δ 33.5. Slow concentration of the mother liquor gave crystals that were suitable for X-ray studies.

Synthesis of [Hg{$Ph_2PC_6H_3$(S-2)($SiMe_3$-3)}$_2$] (6). To a solution of $Ph_2PC_6H_3$(SH-2)($SiMe_3$-3) (0.050 g, 0.136 mmol) and NEt_3 (0.020 g, 0.136 mmol) in methanol (25 mL) was added a solution of mercury acetate (0.021 g, 0.066 mmol) in methanol (5 mL). The solution was stirred at room temperature for several hours, but a solid did not separate. The solvent was removed, and the resulting solid was dissolved in chloroform to yield a compound characterized as [Hg{$Ph_2PC_6H_3$(S-2)($SiMe_3$-3)}$_2$]·$CHCl_3$. Anal. Calcd for $C_{43}H_{45}Cl_3P_2S_2Si_2Hg$ (mol wt 1050.1): C, 49.14, H, 4.32; S, 6.10. Found: C, 50.87; H, 4.58; S, 6.58. IR 3053(m), 2949(m), 2893(m), 1555(m), 1482(m), 1436(m), 1352(s), 1243(m), 1096(m), 853(s), 743(s), 692(s). ^{1}H NMR ($CDCl_3$, ppm): δ 7.8–6.6 (m, 26H), 0.42 (s, 18H). ^{13}C NMR ($CDCl_3$, ppm): δ 138–128. ^{31}P NMR ($CDCl_3$, ppm): 36.1. Crystals of [Hg{$Ph_2PC_6H_3$(S-2)($SiMe_3$-3}$_2$]·$0.75CH_2Cl_2$ suitable for X-ray studies were obtained by crystallization from methanol/dichloromethane.

Synthesis of [EtHg{$Ph_2PC_6H_4$S-2}] (7). To a refluxing solution of $Ph_2PC_6H_4$SH-2 (0.055 g, 0.187 mmol) and NEt_3 (0.026 mL, 0.186 mmol) in methanol (25 mL) was added a solution of ethylmercury(II) chloride (0.055 g, 0.18 mmol) in methanol (15 mL). The solution was stirred at room temperature, and within a few minutes a white solid had formed. The solid was filtered off, washed, dried, and characterized as [EtHg{$Ph_2PC_6H_4$S-2}] (**7**). Anal. Calcd for $C_{20}H_{19}PSHg$ (mol wt 524.0); C, 45.80; H, 3.65; S, 6.10. Found: C, 45.67; H, 3.53, S, 5.96.%. IR (KBr, cm^{-1}): 3067(m), 3054(m), 2967(m), 2935(m), 2850(m), 1583(m), 1477(m) 1433(s), 1419(m), 1396(m), 1170(s), 1094(s), 753(s), 744(s), 719(s), 541(m), 500(m), 466(m). ^{1}H NMR ($CDCl_3$, ppm): δ 7.9–6.6 (m, 14H), 1.8 (q, 2H), 1.5 (t, 3H). ^{13}C NMR ($CDCl_3$, ppm): δ 134–124, 25.1, 15.0. ^{31}P NMR ($CDCl_3$, ppm): δ 17.7. FAB MS: *m*/*z* 522 (M^+). The mother liquor was left to stand and slowly crystallize for several months. Crystals suitable for X-ray studies formed and were identified as [Hg{$Ph_2PC_6H_4$S-2}$_2$] (**5**) and [EtHg{Ph_2P(O)C_6H_4S-2}] (**7***).

Synthesis of [EtHg{Ph_2P(O)C_6H_3(S-2)($SiMe_3$-3)}] (8). Compound **8** was synthesized following a similar procedure as that for **7**, starting from Ph_2P(O)C_6H_3(SH-2)($SiMe_3$-3) (0.164 g, 0.43 mmol), NEt_3 (0.057 mL, 0.43 mmol) in methanol (20 mL), and EtHgCl (0.115 g, 0.43 mmol) in methanol (2 mL). The mixture was stirred, and a white solid formed. The solid was isolated, dried, and characterized as [EtHg{Ph_2P(O)C_6H_3(S-2)($SiMe_3$-3)}] (**8**). Anal. Calcd for $C_{23}H_{27}POSSiHg$ (mol wt 613.1): C, 45.02; H, 4.60; S 5.21. Found: C, 44.95; H, 4.43; S, 5.26%. IR (KBr, cm^{-1}): 3043(m), 2958(s) 2854(m), 1546(m), 1434(s), 1356(s), 1246(m), 1174(s), 1117(m), 1039(m), 856(s), 840(s), 749(m), 691(s). ^{1}H NMR ($CDCl_3$, ppm): δ 7.8–6.5 (m, 13H), 1.8 (q, 2H), 1.4 (t, 3H), 0.5 (s, 9H). ^{13}C NMR ($CDCl_3$, ppm): δ 138–124, 25.4, 14.4, −0.86. ^{31}P NMR

($CDCl_3$, ppm): δ 33.3. FAB MS: m/z 612 (M^+). Slow concentration of the mother liquor gave crystals of [EtHg{$Ph_2P(O)C_6H_3$(S-2)($SiMe_3$-3}]·CH_3OH suitable for X-ray studies.

Synthesis of [{EtHg}$_2${PhP(C_6H_4S-2)$_2$} (9). Compound **9** was synthesized following a similar procedure as that for **7** starting from PhP(C_6H_4SH-2)$_2$ (0.060 g, 0.184 mmol), Et_3N (0.051 mL, 0.36 mmol) in methanol (30 mL), and EtHgCl (0.100 g, 0.370 mmol) in methanol (5 mL). A white solid formed immediately. The solid was isolated, washed with methanol, dried, and characterized as **9**. Anal. Calcd for $C_{22}H_{23}PS_2Hg_2$ (mol wt 784.0): C, 33.75; H, 2.94; S, 8.18. Found: C, 33.55; H, 2.93; S, 8.061%. IR (KBr, cm^{-1}): 3067(m), 3047(m), 3006(m), 2959(m), 1570(m), 1442(s), 1423(s), 1247(m), 1090(s), 749(s), 695(m). ^{1}H NMR ($CDCl_3$, ppm): δ 7.6–6.6 (m, 13H), 1.5 (q, 4H), 1.3 (t, 6H). ^{13}C NMR ($CDCl_3$, ppm): δ 147–125, 25.8(s), 14.9(s). ^{31}P($CDCl_3$, ppm): δ 18.7. FAB MS: m/z 784(M^+); 522 (M − EtHg). Crystallization of the initial product from dichloromethane/methanol gave crystals suitable for X-ray diffraction.

Synthesis of [{EtHg}$_2${PhP(C_6H_3(S-2)($SiMe_3$-3))$_2$}] (10). Compound **10** was synthesized following a similar procedure as that for **7** , starting from PhP{C_6H_3(SH-2)($SiMe_3$-3)}$_2$ (0.080 g, 0.21 mmol), EtN_3 (0.055 mL, 0.38 mmol) in methanol (20 mL), and EtHgCl (0.105 g, 0.396 mmol) in methanol (5 mL). After a few minutes, a white solid formed, and this was filtered off, washed with diethyl ether, dried under vacuum, and characterized as **10**. Anal. Calcd for $C_{28}H_{39}PS_2Si_2Hg_2$ (mol wt 928.1): C, 36.28; H, 4.21; S, 6.91. Found: C, 36.39; H, 4.30; S, 6.44%. IR 3039(m), 2968(m), 2939(m), 1586(m), 1435(s), 1395(m), 1356(s), 1244(m), 1106(s), 846(s), 755(s), 697(m). ^{1}H NMR ($CDCl_3$, ppm): δ 7.9–6.6 (m, 11H), 1.8 (q, 4H), 1.4 (t, 6H), 0.4 (s, 18H). FAB MS: m/z 928 (M^+); 699 (M − EtHg). Slow crystallization over several months from the mother liquor gave crystals of [{EtHg}$_2${PhP(O)(C_6H_3(S-2)($SiMe_3$-3))$_2$}] (**10***) and [Hg(EtHg)$_2${PhP(O)(C_6H_3(S-2)($SiMe_3$-3))$_2$}$_2$] (**11**) suitable for X-ray diffraction.

X-ray Crystallographic Studies. Intensity data sets for all compounds were collected using a Smart-CCD-1000 Bruker diffractometer (Mo Kα radiation, λ = 0.71073 Å) equipped with a graphite monochromator. All crystals were measured at 293 K except compound **1**, which was measured at 150 K. The ω scan technique was employed to measure intensities in all crystals. Decomposition of the crystals did not occur during data collection. The intensities of all data sets were corrected for Lorentz and polarization effects. Absorption effects in all compounds were corrected using the program SADABS.[28] The crystal structures of all compounds were solved by direct methods. Crystallographic programs used for structure solution and refinement were those of SHELX97.[29] Scattering factors were those provided with the SHELX program system. Missing atoms were located in the difference Fourier map and included in subsequent refinement cycles. The structures were refined by full-matrix least-squares refinement on F^2. Hydrogen atoms were placed geometrically and refined using a riding model with U_{iso} constrained at 1.2 (for nonmethyl groups) and 1.5 (for methyl groups) times U_{eq} of the carrier C atom. In compound **2***, the refinement of the oxygen O1 as one full oxygen atom gives a U_{iso} too large in comparison to the rest of the atoms in the complex. However, from a chemical point of view, we do not have any doubt that this position is actually occupied by an oxygen atom. Besides, the P−O distance and the larger P−Cd distance of the carrier phosphorus support this statement. The large U_{iso} suggests that this position is only partially occupied by an oxygen atom. The occupancy parameter for this oxygen was explored using two different approaches. One of them was to refine simultaneously the occupancy and the U_{iso}. Upon convergence, the occupancy parameter obtained was 0.675 and the U_{iso} was 0.09256. A second approach was to fix the U_{iso} at a value of 0.045, which is comparable to the value found in other complexes and to the value of the neighbor atoms. The occupancy parameter obtained was 0.65. So, the second approach should be preferred. This indicates that only the 65% of the molecules in the crystal structure are oxidized. In the remaining nonoxidized 35% of the molecules, the phosphorus atoms are expected to be coordinated to the cadmium atoms. However, the lack of residual electronic density in the vicinity of the phosphorus atom suggests that this unoxidized phosphorus atom is not coordinated to the cadmium atom. This does not seem too likely. All the residual electronic density is around the cadmium atoms so the possibility of further disorder could not be explored. In conclusion, we believe that the unoxidized phosphorus atom of the remaining 35% of the molecules present in the crystal structure should be coordinated to the cadmium atom, but this cannot be proven with the available crystallographic data. Therefore, only the oxidized units will be discussed.

For all structures, except for compound **6**, non-hydrogen atoms were anisotropically refined. The intensity data set for compound **7*** was too weak to allow anisotropic refinement of all non-hydrogen atoms. In this case, only the heavy atoms (Hg, S, and P) were anisotropically refined. Due to the poor quality of the data for compound **7***, geometrical parameters are not discussed, and these data will only be used to show the connectivity around the metal center. In the last cycles of refinement of all structures a weighting scheme was used with weights calculated using the following formula $w = 1/[\sigma^2(F_o^2) + (aP)^2 + bP]$, where $P = (F_o^2 + 2F_c^2)/3$.

Pertinent details of the data collections and structure refinements are collected in Tables 1 and 2. Further details regarding the data collections, structure solutions, and refinements are included in the Supporting Information. ORTEP3 drawings[30] with the numbering schemes used are shown in Figures 1−3 and 5−9.

Crystallographic data (excluding structure factors) for the structures reported in this paper have been deposited with the Cambridge Crystallographic Data Centre as supplementary publication no. CCDC 642063–642072. Copies of the data can be obtained free of charge on application to CCDC, 12 Union Road, Cambridge CB21EZ, UK (fax: (/44) 1223-336-033; e-mail: deposit@ccdc.cam.ac.uk).

Computational Methods. Geometry optimizations of the structures investigated in this study were carried out by density functional theory (DFT) calculations, using the Gaussian03 package[31] and the X-ray crystallographic data as starting points. In particular, we employed the B3LYP method, which combines Becke's three-

(28) Sheldrick, G. M. *SADABS: Program for absorption correction using area detector data*; University of Göttingen: Göttingen, Germany, 1996.

(29) Sheldrick, G. M. *SHELX97 [Includes SHELXS97, SHELXL97, CIFTAB] - Programs for Crystal Structure Analysis*, Release 97-2; Institüt für Anorganische Chemie der Universität: Göttingen, Germany, 1998.

(30) ORTEP3 for Windows. Farrugia, L. J. *J. Appl. Crystallogr.* **1997**, *30*, 565.

(31) Frisch, M. J.; Trucks, G. W.; Schlegel, H. B.; Scuseria, G. E.; Robb, M. A.; Cheeseman, J. R.; Zakrzewski, V. G.; Montgomery, J. A.; Stratmann, R. E. ; Burant, J. C. ; Dapprich, S.; Millam, J. M.; Daniels, A. D.; Kudin, K. N.; Strain, M. C.; Farkas, O.; Tomasi, J.; Barone, V.; Cossi, M.; Cammi, R.; Mennucci, B.; Pomelli, C.; Adamo, C.; Clifford, S.; Ochterski, J.; Petersson, G. A.; Ayala, P. Y.; Cui Q.; Morokuma, K.; Malick, D. K. ; Rabuck, A. D.; Raghavachari, K.; Foresman, J. B.; Cioslowski, J.; Ortiz, J. V.; Stefanov, B. B.; Liu, G.; Liashenko, A.; Piskorz, P.; Komaromi, I.; Gomperts, R.; Martin, R. L.; Fox, D. J.; Keith, T.; Al-Laham, M. A.; Peng, C. Y.; Nanayakkara, A.; Gonzalez, C.; Challacombe, M.; Gill, P. M. W.; Johnson, B. G.; Chen, W.; Wong, M. W.; Andres, J. L.; Head-Gordon, M.; Replogle, E. S.; Pople, J. A. *Gaussian 98*, Revision A.7; Gaussian, Inc.: Pittsburgh PA, 1998.

Table 1. Summary of Crystallographic Data and Refinement for Zinc and Cadmium Compounds

compound	**1***	**2***	**3**
empirical formula	$C_{54}H_{39}P_3OS_6Zn_3$	$C_{74}H_{59}Cd_2NOP_4S_4$	$C_{50}H_{42}N_4P_2S_4Zn_2$
fw	1185.23	1455.14	1019.80
cryst size, mm^3	1.01 × 0.19 × 0.15	0.30 × 0.22 × 0.13	0.31 × 0.13 × 0.11
temp, K	150(2)	293(2)	293(2)
wavelength	0.71073	0.71073	0.71073
cryst syst	triclinic	monoclinic	monoclinic
space group	$P\bar{1}$	$P2(1)/n$	$P2(1)/c$
unit cell dimens			
a, Å	11.292(11)	22.1791(18)	11.283(2)
b, Å	14.233(14)	12.8523(10)	18.627(4)
c, Å	20.05(2)	24.002(2)	23.290(4)
α, deg	109.455(15)	90.00	90.00
β, deg	97.335(16)	101.395(2)	103.548(4)
γ, deg	99.492(16)	90.00	90.00
vol, Å^3	2938(5)	6706(9)	4758.9(15)
Z	2	4	4
μ, mm^{-1}	1.544	0.889	1.290
no. reflns collected	32654	23237	30492
no. independent reflns	11882 [R(int) = 0.0280]	7976 [R(int) = 0.0716]	9748 [R(int) = 0.0427]
data/restraints/params	11882/0/604	7976/0/776	9748/ 0/561
GOF	1.056	0.790	1.049
final R indices [$I > 2\sigma(I)$]	R = 0.0310 wR = 0.0794	R = 0.0415 R_w = 0.0486	R = 0.0380 wR = 0.0817

parameter nonlocal hybrid exchange potential[32] with the nonlocal correlation functional of Lee, Yang, and Parr.[33] The basis set used in the calculations was the standard LanL2DZ, which consists of the Dunning/Huzinaga full double-ζ (D95)[34] for first row and Los Alamos effective core potentials plus double-ζ functions on Na−Bi.[35–37]

Results and Discussion

Zinc and Cadmium Compounds. Zinc and cadmium phosphinothiolate complexes $[Zn\{PhP(C_6H_4S\text{-}2)_2\}]$ (**1**) and $[Cd\{Ph_2PC_6H_4S\text{-}2\}_2]$ (**2**) were easily prepared in good yield by oxidation of a metal anode in a cell containing a solution of the corresponding ligand in acetonitrile and a small amount of tetramethylammonium perchlorate as an electrolytic carrier. The incorporation of pyridine as an additional coligand in the cell allowed the synthesis of mixed complexes such as $[Zn\{PhP(C_6H_4S\text{-}2)_2\}(py)]$ (**3**) and $[Cd\{PhP(C_6H_4S\text{-}2)_2\}(py)]$ (**4**). These compounds were moderately soluble in the reaction solvent and were obtained as air-stable white crystalline solids in the bottom of the cell. The complexes are soluble in chloroform and in a range of other chlorinated organic solvents.

The electrochemical efficiency for these processes, E_f, defined as the number of moles of metal dissolved per faraday of charge, was always close to 0.5 mol F^{-1}. These values, along with the evolution of hydrogen at the cathode, are compatible with the following mechanism:

$$\text{Cathode: } PhP(C_6H_4SH\text{-}2)_2 + 2e^- \rightarrow \{PhP(C_6H_4S\text{-}2)_2\}^{2-} + H_2$$

$$\text{Anode: } M \rightarrow M^{2+} + 2e^-$$

$$\text{Solution: } M^{2+} + \{PhP(C_6H_4S\text{-}2)_2\}^{2-} \rightarrow [M\{PhP(C_6H_4S\text{-}2)_2\}] \quad M = Zn, Cd$$

A similar mechanism can be proposed for the synthesis of metal complexes with the ligand $Ph_2PC_6H_4SH$-2.

The spectroscopic data for **1**–**4** (Experimental Section) are indicative of the presence of the coordinated phosphinothiolate ligands in the complexes. Slow concentration of the mother liquors from the syntheses of complexes **1**, **2**, and **3** yielded crystals suitable for X-ray studies of $[Zn_3\{PhP(C_6H_4S\text{-}2)_2\}_2\{PhP(O)(C_6H_4S\text{-}2)_2\}]$ (**1***), $[Cd_2\{Ph_2PC_6H_4S\text{-}2\}_3\{Ph_2P(O)C_6H_4S\text{-}2\}]\cdot CH_3CN$ (**2***), and $[Zn_2\{PhP(C_6H_4S\text{-}2)_2\}_2(py)_2]\cdot 2CH_3CN$ (**3**). The structural resolutions of **1*** and **2*** show the presence of both phosphinothiolate and oxophosphinothiolate forms of the ligand (*vide infra*). The oxygen in the oxophosphinothiolate moieties in **1*** and **2*** may originate from the incorporation of adventitious oxygen from the solvent during the crystallization process. Such facile oxidations have been observed in other compounds containing this type of ligand.[38]

However, all efforts to isolate crystals of $[Zn\{PhP(C_6H_4S\text{-}2)_2\}]$ (**1**), $[Cd\{Ph_2PC_6H_4S\text{-}2\}_2]$ (**2**), and $[Cd\{PhP(C_6H_4S\text{-}2)_2\}(py)]$ (**4**) were unsuccessful. For this reason, the structures of these compounds were optimized by DFT calculations. The results of these calculations are discussed below.

Description of Structures. Compounds **1***, **2***, and **3** were studied by X-ray diffraction. The crystal parameters, experimental details for data collection, and bond distances and angles for these compounds are provided as Supporting Information.

The molecular structure of $[Zn_3\{PhP(C_6H_4S\text{-}2)_2\}_2\{PhP(O)(C_6H_4S\text{-}2)_2\}]$ (**1***) is shown in Figure 1, together with the atomic numbering scheme adopted. Selected bond distances and angles with estimated deviations are listed in Table 3.

The structure consists of trimeric species in which three zinc atoms are coordinated to two bis(2-mercaptophenyl)phenylphosphine ligands and one bis(2-mercaptophenyl)phenyloxophosphine ligand, with three thiolate sulfur atoms of two different ligands bridging the zinc atoms. This gives rise to the formation of a central six-membered $[Zn_3S_3]$ ring. The ligands are all tridentate, but they show different coordination behavior. A first ligand acts as an OS_2 donor and is coordinated to the Zn(1) atom through O(1) and S(1) and to Zn(2) through S(2). A second ligand behaves as a $P(\mu\text{-}S)_2$ donor with the P(2) atom coordinated to Zn(2) and the two sulfur donors, S(3) and S(4), forming a bridge between two

(32) (a) Becke, A. D. *J. Chem. Phys.* **1993**, *98*, 5648. (b) Becke, A. D. *J. Chem. Phys.* **1992**, *96*, 2155–2160.
(33) Lee, C.; Yang, W.; Parr, R. G. *Phys. Rev.* **1988**, *B37*, 785–789.
(34) Dunning, T. H., Jr.; Hay, P. J. In *Modern Theoretical Chemistry*; Schaefer, H. F., Ed.; PlenumNew York, 1976; Vol. *3*, p 1.
(35) Hay, P. J.; Wadt, W. R. *J. Chem. Phys.* **1985**, *82*, 270–283.
(36) Wadt, W. R.; Hay, P. J. *J. Chem. Phys.* **1985**, *82*, 284–298.
(37) Hay, P. J.; Wadt, W. R. *J. Chem. Phys.* **1985**, *82*, 299–310.
(38) (a) Block, E.; Kang, H. Y.; Ofori-Okai, G.; Zubieta, J. *Inorg. Chim. Acta* **1989**, *166*, 155–157. (b) Pérez-Lourido, P.; Romero, J.; García-Vázquez, J. A.; Sousa, A.; Maresca, K.; Rose, D. G.; Zubieta, J. *Inorg. Chem.* **1998**, *37*, 3331–3336.

Table 2. Summary of Crystallographic Data and Refinement for Mercury Compounds

compound	5	6	7*	8	9	10*	11
empirical formula	$C_{36}H_{28}P_2S_2Hg$	$C_{171}H_{182}Cl_6P_8S_8Si_8Hg_4$	$C_{20}H_{19}OPSHg$	$C_{24}H_{31}O_2PSSiHg$	$C_{22}H_{23}PS_2Hg_2$	$C_{28}H_{39}OPS_2Si_2Hg_2$	$C_{52}H_{68}O_2P_2S_4Si_4Hg_3$
fw	787.23	3981.19	538.97	643.20	783.67	944.04	1629.37
cryst size, mm^3	0.31 × 0.20 × 0.08	0.45 × 0.16 × 0.05	0.53 × 0.05 × 0.05	0.47 × 0.25 × 0.06	0.40 × 0.12 × 0.06	0.66 × 0.36 × 0.33	0.46 × 0.09 × 0.07
temp, K	293(2)	293(2)	293(2)	293(2)	293(2)	293(2)	293(2)
wavelength	0.71073	0.71073	0.71073	0.71073	0.71073	0.71073	0.71073
cryst syst	monoclinic	monoclinic	monoclinic	triclinic	triclinic	monoclinic	monoclinic
space group	*C*2/*c*	*C*2/*c*	*P*2(1)/*c*	$P\bar{1}$	$P\bar{1}$	*P*2(1)/*c*	*P*2(1)/*n*
unit cell dimens							
a, Å	16.322(3)	51.447(4)	12.645(6)	10.0294(18)	8.7029(17)	12.472(3)	11.5787(17)
b, Å	9.2713(16)	11.8702(8)	8.614(4)	11.224(2)	11.429(2)	19.760(5)	28.822(4)
c, Å	20.907(4)	33.296(2)	34.752(16)	12.005(2)	12.764(3)	14.744(4)	20.742(3)
α, deg	90.00	90.00	90.00	99.942(3)	110.978(3)	90.00	90.00
β, deg	98.067(3)	114.6160(10)	96.035(9)	101.184(3)	97.386(3)	111.260(4)	101.891(4)
γ, deg	90.00	90.00	90.00	91.568(3)	100.074(3)	90.00	90.00
vol, $Å^3$	3132.3(9)	18485(2)	3764(3)	1303.3(4)	1141.6(4)	3393.0(15)	6773.5(17)
Z	4	4	8	2	2	4	4
μ, mm^{-1}	5.174	3.656	8.377	6.110	13.690	9.298	7.057
no. reflns collected	4242	83214	31445	14986	9744	20666	42799
no. independent reflns	3192 [*R*(int) = 0.0252]	13353 [*R*(int) = 0.0863]	3939 [*R*(int) = 0.2109]	5327 [*R*(int) = 0.0357]	4608 [*R*(int) = 0.0365]	6923 [*R*(int) = 0.0394]	9715 [*R*(int) = 0.0547]
data/restraints/ params	3192/0/186	13353/4/955	3939/6/223	5327/0/273	4608/0/244	6923/0/325	9715/0/604
GOF	1.087	1.036	1.210	0.998	1.046	0.934	0.940
final *R* indices [$I > 2\sigma(I)$]	$R = 0.0206$ wR = 0.0478	$R = 0.0442$ wR = 0.1021	$R = 0.1507$ wR = 0.3329	$R = 0.0291$ wR = 0.0720	$R = 0.0357$ wR = 0.0690	0.0386 wR = 0.0930	0.0531 wR = 0.1267

metal centers. The third ligand behaves as a PS(*μ*-S) system in that its P(3) and S(6) are coordinated to Zn(3) while the other sulfur acts as a bridge. The presence of an oxophosphine group in one of the ligands leads to different environments around the zinc atoms, [OS_3] for Zn(1) and [PS_3] for both Zn(2) and Zn(3).

Every zinc atom is in a distorted tetrahedral environment with bond angles in the range 132.11(6)°–80.79(6)°. The lower values in this range correspond to donor atoms in five-membered chelate rings. All of the Zn−S bond lengths are similar to one another and are in the range 2.431(2)−2.238(2) Å regardless of the terminal or bridging nature of the sulfur, a situation that indicates the presence of a fairly symmetrical thiolate bridge. These values are comparable to those found in other tetrahedral zinc complexes with thiolate ligands that contain five-membered chelate rings, for example, 2.266 Å (average value) found in [$Zn\{SCH_2CH_2N(CH_3)_2\}_2$].[39] In addition, the Zn−P bond distances, 2.358(2) and 2.437(2) Å, are also close to those found in tetrahedral zinc complexes with tertiary phosphines, for example, 2.376(1) Å (average value) found in [$ZnCl_2(PMe_3)_2$].[40] Both of these bond distances are similar to those found in the compound [$Zn\{Ph_2PC_6H_3(S\text{-}2)(SiMe_3\text{-}3)\}_2$], 2.2791(9) and 2.387(1) Å,

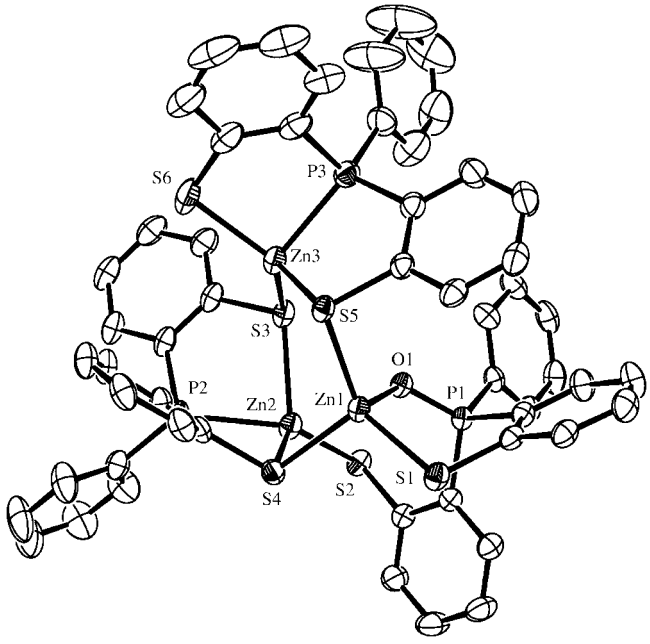

Figure 1. ORTEP diagram of the molecular structure of **1*** with 50% thermal ellipsoid probability.

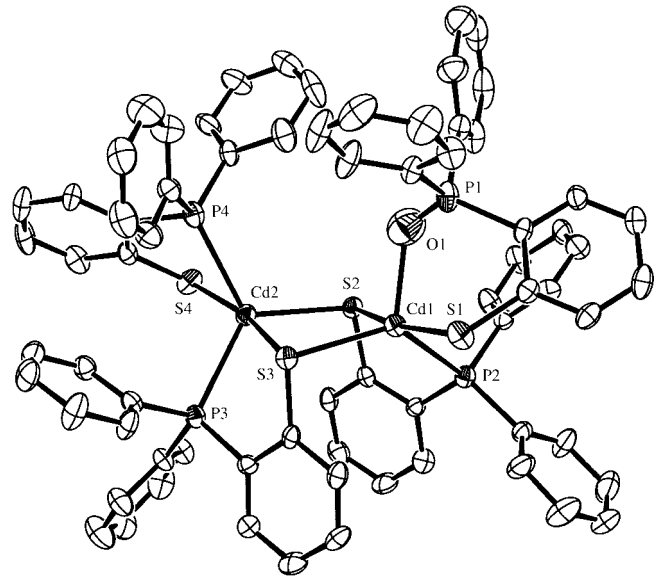

Figure 2. ORTEP diagram of the molecular structure of **2*** with 50% thermal ellipsoid probability.

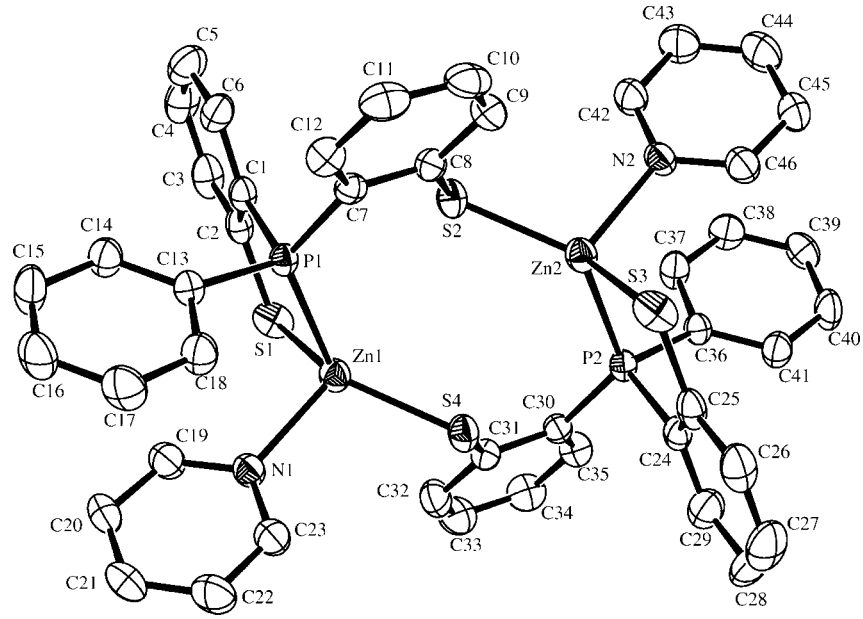

Figure 3. ORTEP diagram of the molecular structure of **3** with 50% thermal ellipsoid probability.

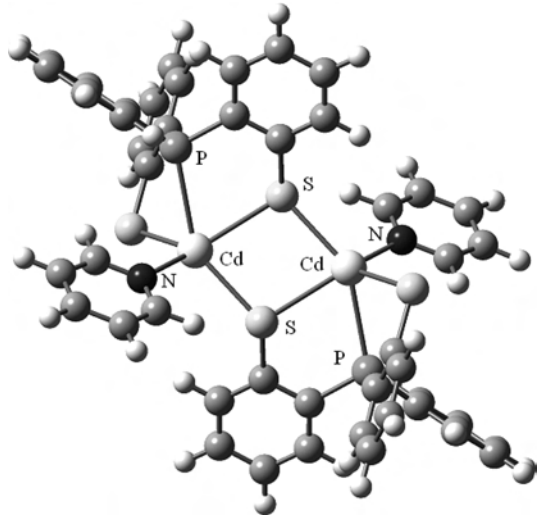

Figure 4. The optimized structure of **4**.

Table 3. Selected Bond Lengths [Å] and Angles [deg] for **1***

Zn(1)−O(1)	2.007(2)	Zn(2)−S(3)	2.431(2)
Z(1)−S(1)	2.2739(15)	Zn(2)−P(2)	2.437(2)
Zn(1)−S(5)	2.3207(17)	Zn(3)−S(6)	2.275(2)
Zn(1)−S(4)	2.3585(17)	Zn(3)−S(3)	2.2910(18)
Zn(2)−S(2)	2.238(2)	Zn(3)−P(3)	2.358(2)
Zn(2)−S(4)	2.3569(18)	Zn(3)−S(5)	2.412(2)
O(1)−Zn(1)−S(1)	102.56(8)	O(1)−Zn(1)−S(5)	104.57(9)
S(1)−Zn(1)−S(5)	123.69(6)	O(1)−Zn(1)−S(4)	99.51(8)
S(1)−Zn(1)−S(4)	109.87(6)	S(5)−Zn(1)−S(4)	112.92(6)
S(2)−Zn(2)−S(4)	122.27(3)	S(2)−Zn(2)−S(3)	113.43(5)
S(4)−Zn(2)−S(3)	113.82(6)	S(2)−Zn(2)−P(2)	132.11(6)
S(4)−Zn(2)−P(2)	86.59(6)	S(3)−Zn(2)−P(2)	80.79(6)
S(6)−Zn(3)−S(3)	122.85(5)	S(6)−Zn(3)−P(3)	91.11(4)
S(3)−Zn(3)−P(3)	118.86(4)	S(6)−Zn(3)−S(5)	111.82(3)
S(3)−Zn(3)−S(5)	118.15(6)	P(3)−Zn(3)−S(5)	84.34(7)

respectively, in which the metal atom is in a $[P_2S_2]$ tetrahedral environment.[25]

A view of $[Cd_2\{Ph_2P(C_6H_4S\text{-}2)\}_3\{Ph_2P(O)(C_6H_4S\text{-}2)\}]$ (**2***) is shown in Figure 2, together with the atomic numbering scheme. Bond lengths and angles with the estimated standard deviations are listed in Table 4. The

Table 4. Selected Bond Lengths [Å] and Angles [deg] for **2***

Cd(1)−O(1)	2.172(7)	Cd(2)−S(2)	2.5232(17)
Cd(1)−S(1)	2.546(2)	Cd(2)−S(3)	2.9684(19)
Cd(1)−S(2)	2.862(2)	Cd(2)−S(4)	2.566(2)
Cd(1)−S(3)	2.5356(16)	Cd(2)−P(3)	2.6270(19)
Cd(1)−P(2)	2.6447(19)	Cd(2)−P(4)	2.674(2)
O(1)−Cd(1)−S(1)	90.3(2)	S(1)−Cd(1)−S(2)	167.21(6)
O(1)−Cd(1)−S(3)	112.06(18)	S(3)−Cd(1)−S(1)	104.66(6)
O(1)−Cd(1)−P(2)	112.24(17)	S(3)−Cd(1)−P(2)	127.45(6)
S(1)−Cd(1)−P(2)	101.90(6)	O(1)−Cd(1)−S(2)	84.8(2)
S(3)−Cd(1)−S(2)	88.13(6)	P(2)−Cd(1)−S(2)	69.35(6)
S(2)−Cd(2)−S(4)	107.87(6)	P(4)−Cd(2)−S(3)	96.47(6)
S(2)−Cd(2)−P(3)	122.24(6)	S(4)−Cd(2)−P(3)	103.64(6)
S(2)−Cd(2)−P(4)	115.91(6)	S(4)−Cd(2)−P(4)	76.42(6)
P(3)−Cd(2)−P(4)	117.86(6)	S(2)−Cd(2)−S(3)	86.04(6)
S(4)−Cd(2)−S(3)	166.01(5)	P(3)−Cd(2)−S(3)	68.72(6)

Table 5. Bond Lengths [Å] and Angles [deg] for **3**

Zn(1)−N(1)	2.124(3)	Zn(1)−S(4)	2.2841(10)
Zn(1)−S(1)	2.2932(11)	Zn(1)−P(1)	2.4172(10)
Zn(2)−N(2)	2.132(3)	Zn(2)−S(2)	2.2760(10)
Zn(2)−S(3)	2.2899(11)	Zn(2)−P(2)	2.3941(11)
N(1)−Zn(1)−S(4)	104.90(8)	N(1)−Zn(1)−S(1)	102.95(8)
S(4)−Zn(1)−S(1)	131.41(4)	N(1)−Zn(1)−P(1)	99.35(8)
S(4)−Zn(1)−P(1)	122.86(4)	S(1)−Zn(1)−P(1)	90.25(3)
N(2)−Zn(2)−S(2)	103.58(8)	N(2)−Zn(2)−S(3)	102.93(8)
S(2)−Zn(2)−S(3)	131.06(4)	N(2)−Zn(2)−P(2)	101.93(8)
S(2)−Zn(2)−P(2)	122.47(4)	S(3)−Zn(2)−P(2)	90.70(4)

structure consists of dimers in which two thiolate sulfur atoms from two ligands bridge the two cadmium atoms. In addition, Cd(1) is coordinated to a phosphorus atom of the bridging ligand and to the thiolate sulfur atom and the oxygen atom of an additional chelating ligand; Cd(2) is coordinated to a phosphorus atom of another bridging ligand and to a sulfur and a phosphorus atom of a chelating ligand. Analysis of the shape-determining bond angles, using the geometrical parameter τ [$\tau = (\beta - \alpha)/60$],[41] gives values of 0.66 and 0.77 and suggests that the cadmium atoms are in distorted

(39) Casals, C. I.; Gonzalez-Duarte, P.; López, C.; Solans, X. *Polyhedron* **1990**, *9*, 763–768.
(40) Cotton, F. A.; Schmid, G. *Polyhedron* **1996**, *15*, 4053–4059.
(41) Addison, A. W.; Rao, T. N.; Reedijk, J.; van Rinj, J.; Verschoor, G. C. *J. Chem. Soc., Dalton Trans.* **1984**, 1349–1356.

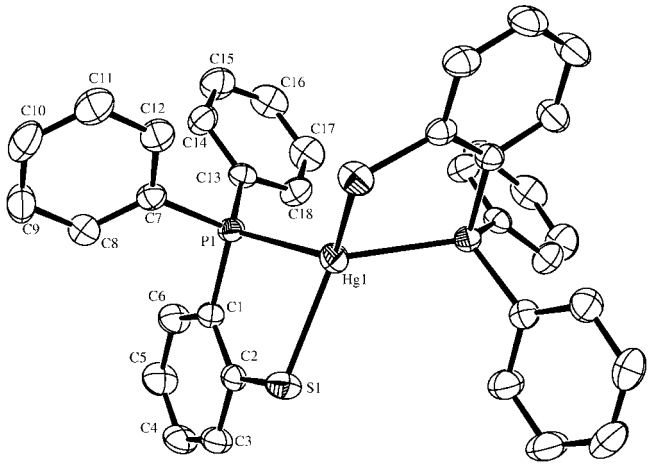

Figure 5. ORTEP diagram of the molecular structure of **5** with 50% thermal ellipsoid probability.

Scheme 1. Schematic Representation of the Routes Employed in the Synthesis of Hg(II) Complexes

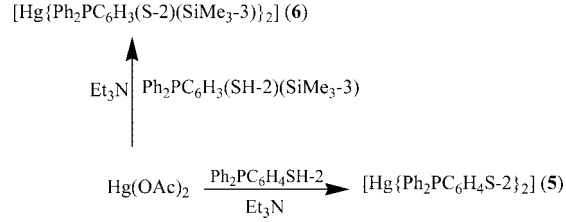

$[CdPOS_3]$ and $[CdP_2S_3]$ trigonal bipyramidal environments with two sulfur atoms in axial sites and O(1), P(2), and S(3) for Cd(1) and P(3), P(4), and S(2) for Cd(2) in the equatorial plane. Angular distortions are observed in the equatorial plane of each cadmium atom, with bond angles in the range 112.06(18)°–127.45(6)°, and along the axial direction of the bipyramid, with angles of 167.21(7)° and 166.01(5)°.

The four-membered ring Cd(1)−S(2)−S(3)−Cd(2) is nearly planar with the two metal atoms 0.1282(6) and 0.1327(7) Å above and the two sulfur atoms −0.1273(6) and −0.1331(7) below the best plane containing the four atoms in question (rms 0.132). The thiolate bridge is clearly asymmetric with two short bond distances, Cd(1)−S(3) 2.5356(16) Å and Cd(2)−S(2) 2.5232(17) Å, and two longer bond distances, Cd(1)−S(2) 2.862(2) and Cd(2)−S(3) 2.9684(17) Å. The latter values are larger than the sum of the covalent radii of tetrahedral cadmium and sulfur atoms, 2.52 Å,[42] and this is indicative of weaker interactions between the metal and these donor atoms. The other bridging bond distances and the cadmium terminal sulfur bond distances, Cd(1)−S(1) 2.546(2) Å and Cd(2)−S(4) 2.566(2) Å, are as expected and are consistent with those found in other dimeric cadmium complexes with pentacoordinated environments around the cadmium and with Cd(μ-SR) bond distances in general.[43] The Cd(1)−O bond distance, 2.172(7) Å, is shorter than those found in other pentacoordinated cadmium complexes involving O-donor ligands, for example, 2.34 Å $[Cd(thiourea)_3(SO_4)]$[44] or 2.387(9) and 2.353(9) Å in dinitrato bis(2-methylmercaptoaniline)Cd(II).[45] The Cd−P bond distances, 2.6270(19) and 2.674(2) Å, are similar to those found in cadmium complexes with tertiary phosphines.[46]

The compound crystallizes with one acetonitrile solvent molecule, which does not interact with the cadmium complex in any significant manner, and there are no noteworthy intermolecular contacts.

The molecular structure of $[Zn_2\{PhP(C_6H_4S\text{-}2)_2\}_2(py)_2]\cdot 2CH_3CN$ (**3**) is shown in Figure 3, together with the atomic numbering scheme adopted. Selected bond distances and angles with estimated deviations are listed Table 5. The structural analysis reveals that the compound is a dimer, with each of the zinc atoms in an $[NPS_2]$ environment formed by a phosphorus atom and a sulfur atom from one ligand, a sulfur atom from the second ligand, and the nitrogen from a pyridine molecule. In this way, each of the ligands acts in a PS chelate manner toward a zinc atom, while the other sulfur atom is used to bind the other metal center. This arrangement gives rise to the formation of a ten-membered ring.

Each Zn atom is in a highly distorted tetrahedral environment with bond angles (Table 5) in the range 131.41(4)°–90.25(3)° for the Zn(1) environment and 131.06(4)°–90.70(4)° for Zn(2). The presence of five-membered chelate rings is the main source of distortion. The bond distances are as one would expect with an average value for the Zn−S distance of 2.2858(10) Å and 2.4172(10) and 2.3941(11) Å for the Zn−P bonds. These values are similar to those found in the previously described zinc compound and also to those in other zinc complexes that contain phosphinothiolato ligands.[25] The Zn−N bond distances, 2.124(3) and 2.132(3) Å, are longer than those reported for several tetrahedral pyridine complexes of zinc(II), in which the Zn−N bond distances are in the range 2.040–2.060 Å.[47] The zinc compound crystallizes with two acetonitrile molecules that are located within the network but do not interact significantly with the complex.

DFT calculations were performed for structural optimizations of complexes **1**, **2**, and **4**. In all cases, the atomic coordinates of the molecules obtained in the crystal structures of the related compounds **1***, **2***, and **3**, respectively, were used as the starting points and references for geometry optimization. In the case of the homoleptic species **1** and **2**, the optimized structures, included in the Supporting Information, are similar to those found in the related compounds **1*** and **2*** by X-ray diffraction. The results for **1** show that the trimer is 35 kcal mol^{-1} lower in energy than the sum of the energy of the monomer and the dimer. Therefore, from the theoretical point of view a structure of trimer should be preferred for **1**. Such trimeric species contains a central Zn_3S_3

(42) Pauling, L. *The Nature of the Chemical Bond*, 3rd ed.; Cornell University Press: Ithaca, NY, 1960; p 246.
(43) Gonzalez-Duarte, P.; Clegg, W.; Casals, I.; Sola, J.; Ruis, J. *J. Am. Chem. Soc.* **1998**, *120*, 1260–1266.
(44) Corao, E.; Baggio, S. *Inorg. Chim. Acta* **1969**, *3*, 617–622.
(45) Griffith, E. A. H.; Charles, N. G.; Rodesiler, P. F.; Amma, E. L. *Polyhedron* **1985**, *4*, 615–620.
(46) (a) Dean, P. A. W.; Payne, N. C.; Vitale, P. J.; Wu, Y. *Inorg. Chem.* **1993**, *32*, 4632. (b) Abrahams, B. F.; Corbell, M.; Dakternieks, D.; Gable, R. W.; Hoskins, B. F.; Tiekimg, E. R. T.; Winter, G. *Aust. J. Chem.* **1986**, *39*, 1993.
(47) (a) Lynton, H.; Sears, M. C. *Can. J. Chem.* **1971**, *49*, 3418. (b) Stephan, W. L.; Palenik, C. J. *Acta Crystallogr.* **1976**, *B32*, 298. (c) Stephan, W. L.; Palenik, C. J. *Inorg. Chem.* **1977**, *16*, 741.

Scheme 2. Schematic Representation of the Routes Employed in the Synthesis of EtHg(II) Complexes

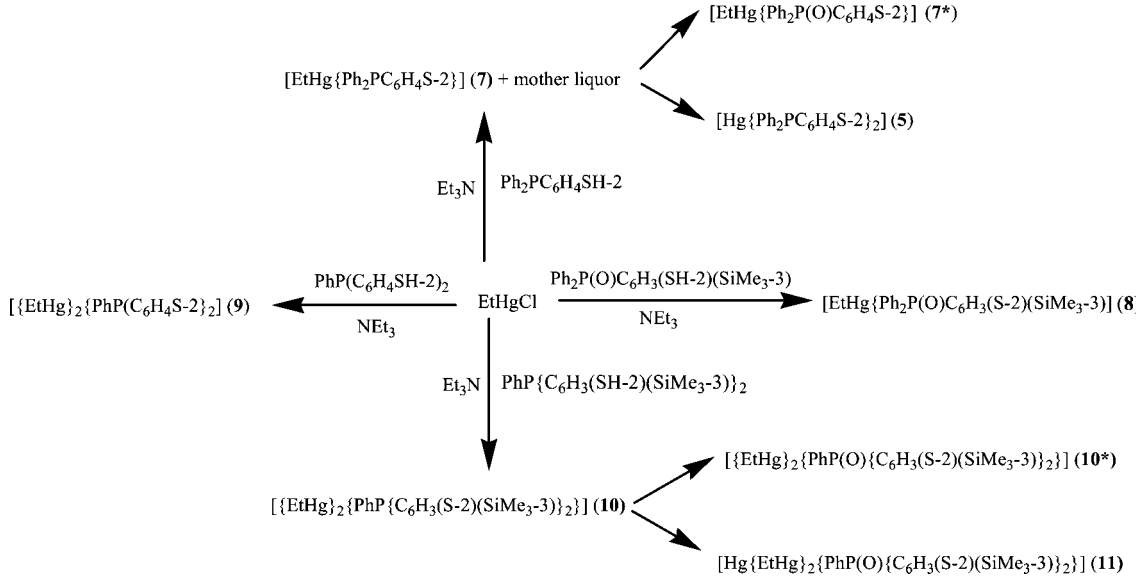

Table 6. Selected Bond Lengths [Å] and Angles (deg) for **5**

Hg(1)−S(1)	2.4986(7)	Hg(1)−P(1)	2.5085(7)
C(2)−S(1)	1.762(3)	P(1)−C(1)	1.808(3)
S(1)−Hg(1)−P(1)	84.28(3)	S(1)−Hg(1)−S(1)[a]	125.47(4)
S(1)−Hg(1)−P(1)[a]	119.24(3)	P(1)−Hg(1)−P(1)[a]	129.77(3)

[a] Symmetry transformation used to generated equivalent atoms: 1, $-x$, y, $-z + 3/2$.

Table 7. Selected Bond Lengths [Å] and Angles (deg) for **6**

molecule A		molecule B	
Hg(1)−S(1)	2.553(2)	Hg(2)−S(3)	2.489(3)
Hg(1)−S(2)	2.512(3)	Hg(2)−S(4)	2.537(3)
Hg(1)−P(1)	2.455(3)	Hg(2)−P(3)	2.492(2)
Hg(1)−P(2)	2.467(2)	Hg(2)−P(4)	2.462(3)
S(1)−Hg(1)−P(1)	81.26(8)	P(4)−Hg(2)−S(3)	126.49(3)
P(1)−Hg(1)−P(2)	137.08(9)	P(4)−Hg(2)−P(3)	127.76(9)
P(2)−Hg(1)−S(2)	83.51(9)	S(3)−Hg(2)−P(3)	84.21(8)
S(1)−Hg(1)−S(2)	111.27(9)	P(4)−Hg(2)−S(4)	82.02(9)
P(1)−Hg(1)−S(2)	122.58(10)	S(3)−Hg(2)−S(4)	118.07(10)
P(2)−Hg(1)−S(1)	123.53(8)	P(3)−Hg(2)−S(4)	123.32(9)

ring with all of the zinc atoms having the same $[PS_3]$ tetrahedral environment. In the case of compound **2**, the optimized structure is dimeric and is similar to that of **2***, with two sulfur atoms acting as bridges and the cadmium centers in pentacoordinated $[P_2S_3]$ environments.

The structure of the mixed complex **4**, Figure 4, shows the presence of dimeric species in which the ligand acts in a terdentate manner, with the sulfur atom acting as a bridge and the other as a terminal atom. In this case, the cadmium is in a pentacoordinate $[PS_3N]$ environment. It is worth noting in this case that the geometry of **4** and the coordination of the ligand are clearly different from those found in zinc complex **3**, which has an analogous composition.

Mercury(II) and Ethylmercury(II) Compounds. The reaction of mercury(II) acetate with $Ph_2PC_6H_5SH$-2 and $Ph_2PC_6H_3$(SH-2)($MeSi_3$-3) in methanol in the presence of triethylamine led to the formation of solids for which the analytical data are consistent with $[Hg\{Ph_2PC_6H_4S\text{-}2\}_2]$ (**5**) and $[Hg\{Ph_2PC_6H_3(S\text{-}2)(SiMe_3\text{-}3)\}_2]\cdot CHCl_3$ (**6**) (Scheme 1).

The spectroscopic data confirm the presence of the coordinate ligands in both complexes. The room temperature ^{31}P NMR spectrum shows a single peak at δ 33.5 and 36.1 ppm for **5** and **6**, which are consistent with data reported for four-coordinate phosphine mercury complexes[48] and show that in solution the ligand is coordinated through the phosphorus atom as confirmed by X-ray diffraction studies (*vide infra*).

The routes employed in the synthesis of ethylmercury complexes are shown in Scheme 2. The reaction of ethylmercury chloride with $Ph_2PC_6H_4SH$-2 in the presence of triethylamine gave a white solid, the analytical data of which are consistent with the formula $[EtHg\{Ph_2PC_6H_4S\text{-}2\}]$ (**7**).

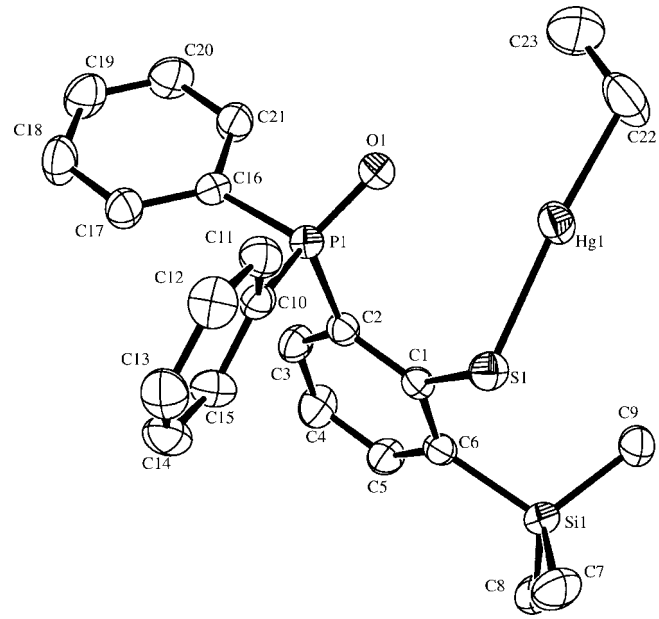

Figure 6. ORTEP diagram of the molecular structure of **8** with 50% thermal ellipsoid probability.

Table 8. Selected Bond Lengths [Å] and Angles (deg) for **8**

Hg(1)−S(1)	2.3739(12)	Hg(1)−C(22)	2.076(6)
P(1)−O(1)	1.483(3)	C(1)−S(1)	1.779(4)
C(22)−Hg(1)−S(1)	175.2(2)		

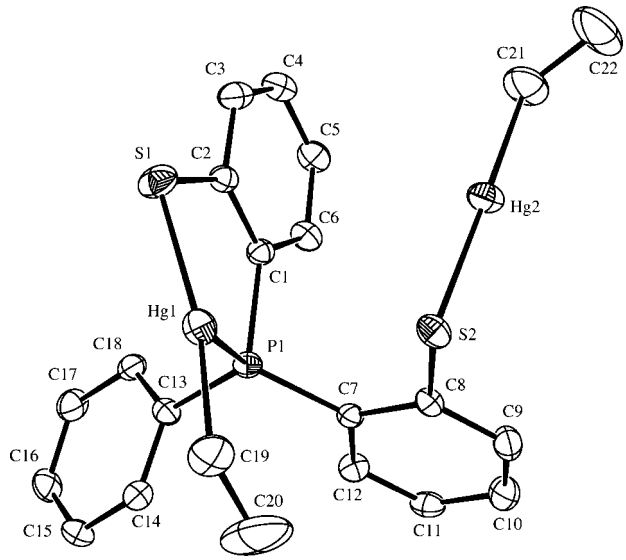

Figure 7. ORTEP diagram of the molecular structure of **9** with 50% thermal ellipsoid probability.

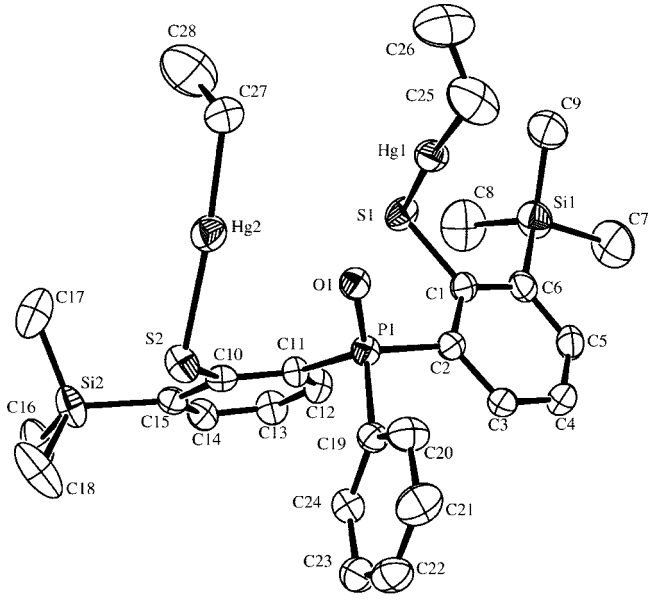

Figure 8. ORTEP diagram of the molecular structure of **10*** with 50% thermal ellipsoid probability.

The IR and NMR studies are compatible with the formula proposed. We were unable to obtain crystals of **7** suitable for X-ray studies, but the structure was optimized using theoretical methods, and the results are shown below. Concentration of the mother liquors from the reaction mixture gave two new compounds. The major isolated component was [EtHg{$Ph_2P(O)C_6H_4S$-2}] (**7***), the structure of which was determined by X-ray diffraction (*vide infra*). A second crystalline compound was obtained from the same solution and X-ray analysis (*vide infra*) confirmed this to be [Hg{$Ph_2PC_6H_4S$-2}$_2$], the preparation of which from mercury acetate has already been described above, and contains a mercury atom coordinated to two monoanionic bidentate ligands. The formation of this compound suggests the occurrence of a cleavage process on the C−Hg bond in the organomercury

(48) Allam, T.; Goel, R. G. *Can. J. Chem.* **1984**, *62*, 615.

Table 9. Selected Bond Lengths [Å] and Angles (deg) for **9** and **10***

9		**10***	
Hg(1)−S(1)	2.386(3)	Hg(1)−S(1)	2.390(2)
Hg(1)−P(1)	2.807(2)	Hg(2)−S(2)	2.362(2)
Hg(2)−S(2)	2.368(2)	Hg(1)−C(25)	2.108(10)
C(19)−Hg(1)−S(1)	166.2(3)	Hg(2)−C(27)	2.067(10)
S(1)−Hg(1)−P(1)	80.27(7)	C(25)−Hg(1)−S(1)	174.0(4)
C(19)−Hg(1)−P(1)	111.6(3)	C(27)−Hg(2)−S(2)	175.7(3)
C(21)−Hg(2)−S(2)	178.7(3)		

Table 10. Selected Bond Lengths [Å] and Angles (deg) for **11**

Hg(1)−S(1)	2.372(4)	Hg(1)−C(25)	2.099(15)
Hg(2)−S(3)	2.380(4)	Hg(2)−C(51)	2.131(18)
Hg(3)−S(2)	2.326(4)	Hg(3)−S(4)	2.328(4)
C(25)−Hg(1)−S(1)	177.9(5)	C(51)−Hg(2)−S(3)	178.3(6)
S(2)−Hg(3)−S(4)	169.45(13)		

starting material. It has been demonstrated that the coordination of organomercury derivatives by strongly chelating ligands polarizes and activates the carbon−mercury bond for protonolysis under these mild conditions.[20–23]

The analytical data for the compound obtained in the reaction between ethylmercury chloride and $Ph_2P(O)C_6H_3$(SH-2)(Me_3Si-3) are consistent with the formula [EtHg{$Ph_2P(O)$-C_6H_3(S-2)(Me_3Si-3)}] (**8**). A study of a solution of this compound indicated its stability, as evidence for cleavage processes was not observed in this case. The ^{1}H NMR spectrum shows characteristic signals for the ligands coordinate, and the single signal at δ 33.3 ppm in the ^{31}P spectrum can be assigned to the presence of a PO group that is not coordinated to the metal. These data all demonstrate that in solution the complex has the same structure as in the solid state, as established by X-ray diffraction (*vide infra*).

The chemistry of the related tridentate ligand PhP(C_6H_4SH-2)$_2$ was also investigated in order to evaluate the influence of ligand denticity on the reaction chemistry and product identity. The reaction of this ligand with ethylmercury chloride in methanol in the presence of Et_3N gave a white solid, the analytical data of which are consistent with a compound of general formula [{EtHg}$_2${PhP(C_6H_4S-2)$_2$}] (**9**). The spectroscopic data confirm the presence of a coordinated ligand and evidence for oxidized phosphorus atoms was not seen. NMR ^{31}P spectrum again shows a relatively broad signal at δ 18.7 ppm, which can be assigned to the phosphorus atom coordinated to mercury. These data confirm the structure found by X-ray diffraction in the solid state.

The reaction between EtHgCl and PhP{C_6H_3(SH-2)($SiMe_3$-3)}$_2$ initially gave an insoluble white solid in the reaction medium. The analytical data for this compound are consistent with the formula [{EtHg}$_2${PhP(C_6H_3(S-2)($SiMe_3$-3))$_2$}] (**10**). The spectroscopic data confirm the presence of the coordinated ligand, and the FAB spectrum shows a molecular ion peak at *m*/*z* 928. Crystals of **10** suitable for X-ray diffraction could not be obtained, and the structure of this compound was optimized by DFT calculations. The results of these calculations are shown below. Crystallization of the compound discussed above gave two different products. In the first product, oxidation of the phosphorus atom of the ligand had occurred and led to the formation of [{EtHg}$_2${PhP(O)(C_6H_3(S-2)($SiMe_3$-3))$_2$}] (**10***). The crystal structure of this compound

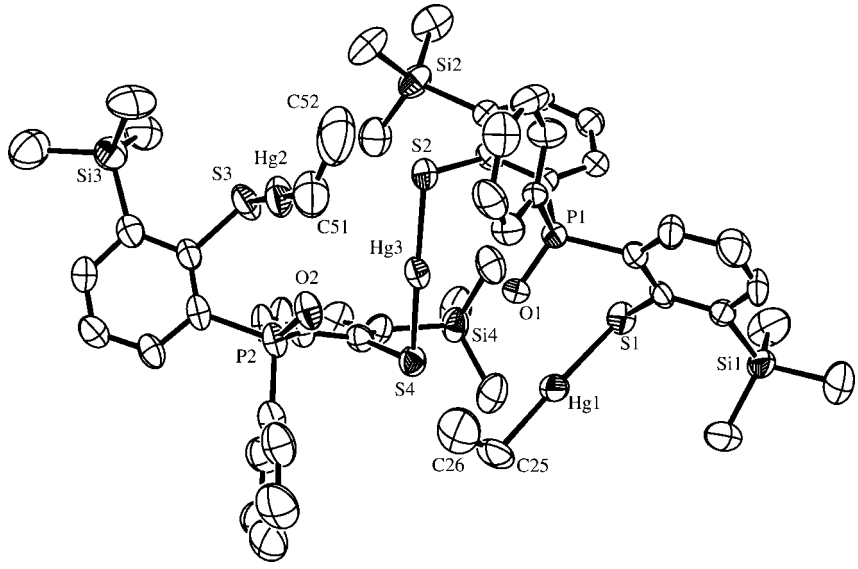

Figure 9. ORTEP diagram of the molecular structure of **11** with 50% thermal ellipsoid probability.

was studied by X-ray diffraction (*vide infra*) and was found to be similar to that of compound **9**. The crystallization process also gave a minor component. X-ray analysis (*vide infra*) of this compound showed the presence of a species of formula $[Hg\{EtHg\}_2\{PhP(O)(C_6H_3(S\text{-}2)(SiMe_3\text{-}3)_2\}_2]$ (**11**). In this case, cleavage of the Hg−C bond had taken place.

Description of the Structures. The molecular structure of $[Hg\{Ph_2PC_6H_4S\text{-}2\}_2]$ (**5**) is shown in Figure 5. The compound possess a 2-fold rotation axis that passes through the mercury atom. Selected bond distances and angles are given in Table 6. The asymmetric unit of compound $Hg\{Ph_2PC_6H_3(S\text{-}2)(SiMe_3\text{-}3)\}_2]$ (**6**) contains two molecules of the complex and 1.5 molecules of CH_2Cl_2, and the molecular structure of one of the two molecules is included in the Supporting Information. Selected bond distances and angles are given in Table 7.

Both compounds consist of discrete molecules in which the mercury atoms are coordinated to two monoanionic bidentate (η^2-P,S) ligands. The geometry around the metal in both cases is distorted tetrahedral with bond angles corresponding to five-membered chelate rings, 84.28(3)° in **5** and 82.38(9)° (average value) in **6**.

The Hg−S bond distances, 2.4986(7) Å for **5** and 2.523(3) Å (average value) for **6**, are very similar to one another and close to those found in other mercury thiolates in which the metal atom is tetracoordinated in a tetrahedral environment, for example, 2.537(1) and 2.552(1) Å in $[Hg(SC_6H_4Cl)_4]^{2-}$[49] or 2.543(7) Å in $[(np_3)Hg(SC_6H_4CH_3)]^+$ (np_3 = $N(CH_2CH_2PPh_2)_3$).[20] The Hg−P bond distances are relatively short at 2.5085(7) and 2.469(3) Å (average value) for **5** and **6**, respectively. These values are slightly shorter than those found in $[(np_3)Hg(SC_6H_4CH_3)]^+$, which are in the range 2.593(7)–2.633(8) Å, and in $[HgX_2(PPh_3)_2]$ complexes, which are in the range 2.45–2.91 Å.[50]

The structure of one of the two molecules of $[EtHg\{Ph_2P(O)\text{-}C_6H_4S\text{-}2\}]$ (**7***) in the asymmetric unit is include in the Supporting Information. Unfortunately, the X-ray diffraction data are of poor quality, and for this reason, the structure is shown only to demonstrate the connectivity of the atoms around the metal center (see X-ray Crystallographic Studies). As a result, the geometrical parameters for this compound will not be discussed. The molecular structure of $[EtHg\{Ph_2P(O)C_6H_3(S\text{-}2)(Me_3Si\text{-}6)\}]\cdot CH_3OH$ (**8**) is shown in Figure 6, together with the atomic numbering scheme adopted. A selection of bond distances and angles for this complex are given in Table 8.

The structures of both compounds are similar consisting of monomeric species in which the mercury is coordinated to a carbon atom of the ethyl group and the thiolate sulfur of the ligand. In both compounds, the geometry around the metal atom is essentially linear with S−Hg−C bond angles close to the ideal value of 180°. The Hg−C bond length, 2.076(6) Å, and the Hg−S bond length, 2.3739(12) Å, for **8** are within the expected range for linear organomercury compounds coordinated with thiolate ligands.[51,52] The value of the distance between the mercury atom and the oxygen atom of the oxophosphine ligand, 2.713 Å, is larger than the normal covalent bond between the two atoms, 2.00–2.30 Å,[53] but is shorter than the sum of the van der Waals radii, 3.00–3.23 Å,[54] and may be considered as indicative of some interaction.[55] Compound **8** crystallizes with a molecule of methanol, which maintains a hydrogen-bonding interaction with the oxygen atom of the ligand.

(49) Choudhury, S.; Dance, I. G.; Guerney, P. J.; Rae, A. D. *Inorg. Chim. Acta* **1983**, *70*, 227–230.

(50) Guergi, H. B.; Fischere, E.; Kunz, R. W.; Parvez, M.; Pregosin, P. S. *Inorg. Chem.* **1982**, *21*, 1246–1256.

(51) Castiñeiras, A.; Hiller, W.; Strahle, J.; Bravo, J.; Casas, J. S.; Gayoso, M.; Sordo, J. *J. Chem. Soc., Dalton Trans.* **1986**, 1945–1948.

(52) Block, E.; Brito, M.; Gernon, M.; McGowty, D.; Zubieta, J. *Inorg. Chem.* **1990**, *29*, 3172–3181, and references therein.

(53) (a) Taylor, N. J.; Wong, Y. S.; Chieh, P. C.; Carthy, A. J. *J. Chem. Soc., Dalton Trans.* **1975**, 438–442. (b) Dittmar, G.; Hellmer, E. *Angew. Chem., Int. Ed. Engl.* **1969**, *8*, 679.

(54) (a) Grdenic, D. *Q. Rev.* **1965**, 303–328. (b) Bondi, A. *J. Chem. Phys.* **1964**, *68*, 441–451.

(55) Barbaro, P.; Ghilardi, C. A.; Midollini, S.; Orlandini, A.; Ramirez, J. A.; Scapacci, G. *J. Organomet. Chem.* **1998**, *555*, 255–262.

The molecular structures of [{EtHg}$_2${PhP(C$_6$H$_4$S-2)$_2$}] (**9**) and [{EtHg}$_2${PhP(O){C$_6$H$_3$(S-2)$_2$(SiMe$_3$-3)}$_2$}] (**10***) are shown in Figures 7 and 8, along with the atom labeling schemes. Selected bond distances and angles are given in Table 9. The two structures can be considered to be related, although the presence in the second compound of an oxidized phosphorus atom gives rise to structural differences between the two complexes. In compound **9**, the two mercury atoms have different coordination behavior and different geometries. The Hg(2) center is coordinated in a linear manner to a carbon from the ethyl group and a sulfur atom, with a C−Hg−S(2) bond angle of 178.7(3)°.

Compound **10*** consists of two EtHg− units that are bonded to two thiolate sulfur atoms from the dianionic ligand. Both mercury atoms have a linear coordination in which the metal is only bonded to a carbon atom from the ethyl group and the anionic sulfur. The oxygen atoms from the PO groups are sufficiently remote that the existence of interactions with the mercury atom can be ruled out.

The bond distances in the S−Hg−C fragment are as one would expect for covalent bonds. However, the Hg(1) atom, in addition to the strong covalent Hg−C and Hg−S bonds, is also linked to the phosphorus atom of the ligand. The Hg−P bond distance is 2.807(2) Å, which is shorter than the sum of the van der Waals radii of mercury and phosphorus[42] (3.4 Å) and is characteristic of the presence of a weak interaction.[56] In this case, the C−Hg−S bond angle is closed and has a value of 166.2(3)°, the lowest value in the organomercury compounds discussed here and characteristic of complexes in which secondary coordination occurs.

The molecular structure of [Hg{EtHg}$_2${PhP(O)(C$_6$H$_3$(S-2)(SiMe$_3$-3))$_2$}$_2$ (**11**) is shown in Figure 9 along with the atom labeling scheme. Selected bond distances and angles are given in Table 10. The compound is trinuclear and contains mercury atoms of different natures. The atoms Hg(1) and Hg(2) are coordinated in a linear fashion with a carbon atom of the ethyl group and the sulfur of a phosphinothiolate ligand. In addition, the oxygen atom from the PO group of the ligand is 2.622(7) and 2.674(9) Å away from the mercury, a situation that seems to indicate the presence of a weak interaction between these atoms. The Hg(3) atom is coordinated in a linear manner with two sulfur atoms from different thiolate ligands, and there are also weak interactions with the oxygen atoms of the two ligands, bond distances 2.617(7) and 2.689(8) Å, in a coordination that can be considered as 2 + 2, which is characteristic of some Hg(II) compounds. In all three cases, regardless of the presence of possible secondary interactions, the bond angles around the metal are in the range 169.45(13)°–178.3° and Hg−S bond distances in the range 2.326(4)–2.380(4) Å, values similar to those found in the previously described mercury compounds, and therefore do not warrant further discussion.

The structures of **7** and **10** were optimized by DFT calculations. The results obtained are shown in the Supporting Information. In these compounds, and in relation to the structures of compounds **7*** and **10***, the presence of a bonding interaction can be seen between the metal and the phosphorus, which in this case is not oxidized. This situation is consistent with the softer character of this atom. Whereas the structures of complexes **7*** and **10***, obtained by X-ray diffraction, have the mercury in a digonal coordination, in **7** the metal center is tricoordinated and in **10** the two mercury atoms have different environments, with one coordinated to the phosphorus of the ligand.

Acknowledgment. This work was supported by Xunta de Galicia (Spain) and by the Ministerio de Ciencia y Tecnología (Spain) (Grant No. CTQ2006-05298).

Supporting Information Available: Crystallographic data in cif format, optimized structures of **1**, **2**, **7**, **10**, and ORTEP diagrams of **6** and **7***. This material is available free of charge via the Internet at http://pubs.acs.org.

IC7005925

(56) Cecconi, F.; Ghilardi, C. A.; Ienco, A.; Midollini, S.; Orlandini, A. *J. Organomet. Chem.* **1999**, *575*, 119–125.